Subsea buoyancy and gravity energy storage system for deep-water applications
A preliminary assessment

Novgorodcev, Andre R.; Mols, Frank; Laguna, Antonio Jarquin

DOI
10.1115/OMAE2022-80422

Publication date
2022

Document Version
Final published version

Published in
Ocean Renewable Energy

Proceedings of the ASME 2022 41st International Conference on Ocean, Offshore and Arctic Engineering
OMAE2022
June 5-10, 2022, Hamburg, Germany

OMAE2022-80422

SUBSEA BUOYANCY AND GRAVITY ENERGY STORAGE SYSTEM FOR DEEP-WATER APPLICATIONS: A PRELIMINARY ASSESSMENT

Andre R. Novgorodcev Jr.
Offshore Engineering
Delft University of Technology
Delft, The Netherlands
A.R.NovgorodcevJunior@tudelft.nl

Frank Mols
Offshore and Dredging Engineering
Delft University of Technology
Delft, The Netherlands
frank.mols@live.nl

Antonio Jarquin Laguna
Offshore and Dredging Engineering
Delft University of Technology
Delft, The Netherlands
A.JarquinLaguna@tudelft.nl

ABSTRACT

This article presents a preliminary assessment of a subsea buoyancy and gravity energy storage system (SBGESS). The storage device is designed to power an off-grid subsea water injection system to be installed at the Libra oil field in Brazil at 2000 m below sea level. Two 12MW floating wind turbines provide the energy supply. The system performance is evaluated according to historical wind data from reanalysis models, the water injection pumps' power curves, the required daily water flow rate, and the maximum number of shutdowns allowed per year. A control strategy with three different operation modes and one energy-save sub-mode was implemented to optimise the size of the proposed energy storage system.
Keywords: Gravity energy storage; Buoyancy energy storage; offshore energy

INTRODUCTION

The fast uptake in penetration of renewable energies in combination with new environmental policies will require reductions in the production costs and emissions from the oil and gas (O&G) industry [1]. Particularly in offshore oil production, two central technology routes are being considered. The first one is the relocation of part of the oil processing equipment to the seabed to reduce the size of the platforms and increase the process efficiency, potentially reducing the CAPEX costs up to 20% [2]. A variety of subsea equipment is in the operation or development phase for water depths up to 3000 m with a range of energy consumption of a few hundred kW to 18 MW [3]. An example of such equipment is the SPRINGS® (Subsea PRocessing and INjection Gear for Seawater), which can replace a top deck water treatment and injection system with a 17% reduction in the CAPEX [4].

The second alternative is the adoption of renewable energies to reduce the internal consumption of oil and gas, representing 5% of the field's gross production [1]. The advantages of adopting renewable energy are both environmental and economic, as the life cycle cost of offshore renewables is getting closer to the cost of conventional generation technologies. This difference can eventually disappear if carbon taxes are applied. Two case studies showing the theoretical cost reduction are presented by [5], while a practical example of this integration has been shown in the Hywind Tampen project in Norway [6].

For offshore applications, one of the main difficulties faced by renewable sources is that they are intermittent by nature, requiring a backup source of power to ensure continuous operation. Access to this backup power source is particularly challenging for autonomous subsea equipment that does not have access to an electrical connection from a power grid or platform. In this case, the use of an energy storage system is required to comply with the system's energy demand.

Energy storage system

Wang et al. [7] presented a review of the energy storage technologies for offshore applications. The present work will focus on using potential gravitational energy for medium and long-time applications (from hours to days scale). Nowadays, this approach

represents 94% of the total energy storage capacity worldwide in the form of Pumped Hydro Storage (PHS). However, only a few concepts are being considered for deep water applications.

In the Submerged PHS (SPHS) concepts, the energy is stored by pumping the water from a submerged reservoir for charging and letting the ocean's hydrostatic pressure fill it with water for discharge. These reservoirs could be concrete spheres [8, 9] or a bank of steel pipes [10]. Independently of the reservoir's material, the energy storage capacity increases proportionally with the water depth. In contrast, the walls' thickness and, consequently, the costs increase as a function of the material and the geometry. The cited authors have no consensus on the technical-economical limitations regarding the SPHS's water depth, which varies between 750 [8] and 2000 meters [10], limiting the deployment potential for ultra-deep water applications.

Another storage option is the gravitational storage system (GES), which relies on the same principle of the PHS but utilises weights instead of water to store potential energy. Unlike onshore developments that already have some operating prototypes, limited scientific publications were found on offshore GES. In [11–14], the use of platforms or barges to lift cylindrical bodies of 100 tonnes or more from up to 4000 m water depth is proposed. The lifted weights are then connected to surface floaters linked to a mooring structure installed a few meters below the surface; in this way, a crane could repeat the operation, increasing the total energy storage capacity. The main limitation of such systems is the high cost associated to the required mooring in order to maintain the lifted weights at a stable position during extreme weather conditions, limiting the applicability in places susceptible to these conditions [14]. The advantages are the theoretical round trip efficiency of up to 85%, the modularity and the relatively low cost per MWh [7, 14].

Buoyancy energy storage (ByES) utilises the buoyancy forces to store potential energy. There are two main concepts of ByES. The first [15] consists of a floating structure with a fluid reservoir that is drained and consequently raised to store energy. In the discharge mode, water is allowed to pass through a turbine to fill the reservoir and lower the system. The second concept consists of floating bodies forced down by a cable to store energy [16–18]. The movement is reversed for power generation. The cable could be connected to a hoist drum mounted on the seabed or rigged through a pulley to reach a surface mounted hoist. Modelled blocks of floating materials like Styrofoam [17] or gas-filled vessels [16] are used as floaters. The theoretical maximum efficiency for the ByES is reported at 83% [7].

An innovative energy storage system that combines buoyancy and gravitational energy storage devices installed in a single semi-submerged support structure is proposed in this work and represented in Fig. 1. In this schematic, the orange dotted lines represent the power cables, the solid grey the traction cables, and the dashed black the mooring lines. The semi-sub structure is shown in red, and the floaters and weights in blue. This system

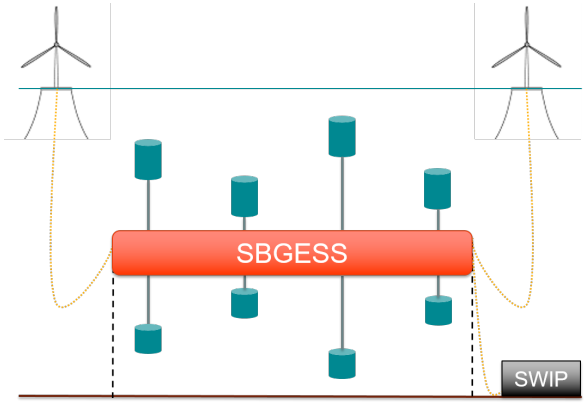

FIGURE 1. SCHEMATIC OF THE SUBSEA BUOYANCY GRAVITY ENERGY STORAGE SYSTEM (SBGESS), ARTIST IMPRESSION.

is referred to as Subsea Buoyancy Gravity Energy Storage System (SBGESS).

These two technologies were selected due to their capacity to store considerable high amounts of energy, with a cycle efficiency above 80% and a physical operation based on a relatively simple mechanical principle. In this concept, the floaters and weights are connected to drum hoists mounted side by side. During the charging process, the hoists will simultaneously retrieve and lift the floaters and weights, compensating the resultant vertical forces acting on the support structure. Similarly, the discharge process can take place when the hoist motor is inverted. The resulting neutral vertical force simplifies the system's design requirements by eliminating the need of an active ballasting control to maintain structural stability during operation, which is the case in other offshore GES concepts. Being semi-submerged, the associated costs with keeping a stable position during extreme weather conditions is expected to be lower compared to surface solutions and thus unlocking the potential of deployment areas.

Each set of weight, floater and electrical and mechanical equipment is referred as a single energy storage module (ESM). The power for each module is determined by the torque exerted by the cable and the rotational speed of the hoist drum. In order to reduce the vertical drag forces acting on the weights and floaters, smaller velocities values are considered while adjusting the acting forces to regulate the power. The total energy stored is a function of the length of the cables and the number of modules. This modular approach allows for wider flexibility regarding energy storage capacity of the system.

Case study

The SBGESS could be applied in high productivity oil fields located on ultra-deep waters like the Libra in Santos Basin, Brazil. The oil field is located 160 km offshore from Rio de

Janeiro State, with an average water depth of 2000 m without an available electrical or grid connection. This pre-salt field has an estimated 8 to 12 billion barrels of oil equivalent reserves [19]; however, the high gas-oil rate of 450 Nm^3/m^3 combined with a CO_2 content of about 45% poses a big challenge. The CO_2 separation and reinjection plant occupies 60% of the deck space of the floating production storage and offloading unit [20]. This plant is also responsible for a significant fraction of the total energy consumption and requires a continuous operation.

One of the solutions to liberate space and energy to increase the platform's processing capacity is to utilise an externally powered seabed mounted water injection plant (SWIP). Unlike the CO_2 separation and reinjection process, the water injection does not require to provide constant flow rate (although the efficiency and production might be compromised from large power fluctuations), making it more suitable to operate in combination with renewable energy sources. The SWIP is considered to have the same average capacity as a typical water injection system with 496.85 m^3/h (75000 BPD) [21]. Monthly or yearly deviations from this value are allowed, but may reduce the production during that period. The system could be replaced by two SPRINGS systems of 42000 BPD each [4]. The pumps used in the SWIP are designed to be in a 1 to 3 MW range [22]. In this study, each pump will be operating with a rotational speed between 1500 and 4440 rpm with a rated shaft power of 2170 kW [21]. The pumps use a variable speed drive and have a soft-starter function, making them highly suitable to operate under alternating power supply conditions. Based on industrial experience the number of stops per year is limited to 70 events to ensure the reliability of the pumps [21].

According to [23], wind energy is the most suitable renewable source for this site considering technical, economic, and environmental aspects. A preliminary assessment of an SBGESS is made, considering that floating wind turbines will power a SWIP. Despite the turbulent nature of the wind resource, the large rotor's inertia of the wind turbines allow to smooth out short period power fluctuations (sub-minute scale) provided to the SWIPs. In addition, flywheels could be attached to the pump's axes to further increase the rotational inertia, so the SBGESS could be designed to account for longer time power fluctuations.

METHODOLOGY

The employed methodology to determine the capacity of the weights (GES) and floaters (ByES) is visualised in Fig. 2. First, the wind speed and statistics for the proposed location were analysed. In combination with the power curves from the selected wind turbines, an expected energy yield was obtained. The energy demand from the SWIP was evaluated based on an approximation of the transmission's efficiency and the pump's performance. With this information, a simulation of the supplied water injection was performed using hourly values. An iterative process was introduced to account for the required energy storage capacity at each hourly time step. The model is not able to deal with time-scales in the order of seconds, which limits its application to average values of flow rate water injection neglecting transient effects of the operating weights and floaters.

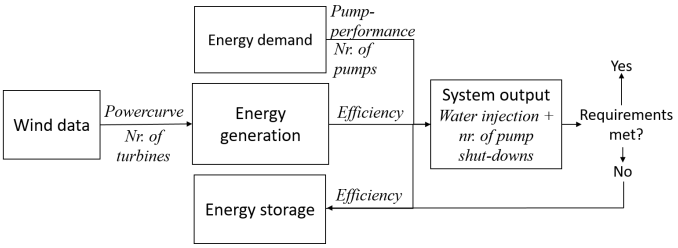

FIGURE 2. OVERVIEW OF THE METHODOLOGY TO DETERMINE THE REQUIRED ENERGY STORAGE CAPACITY AND POWER OF THE PROPOSED SBGESS.

Energy yield

Historical wind data was obtained from the Copernicus climate data project [24] and interpolated for the location corresponding to the middle point of the western part of the Libra field at Lat -24.5 and Long -42.2. The data consist of hourly values of the wind speed in u and v direction at 100 m height over 41 years (1979 - 2019) using reanalysis models [25].The empirical power-law vertical profile was used to adjust the wind velocities of reanalyses data to the required hub heights of the wind turbines according to Eqn. (1). Compared to the logarithmic scaling, the power-law expression gives a more accurate approximation for offshore wind speeds at higher heights [26]. The influence of the atmospheric stability on the vertical profile was not included in this approach.

$$C_{150m} = C_{100m}\left(\frac{z_{150m}}{z_{100m}}\right)^{\alpha_{shear}} \tag{1}$$

Where:

C_{150m} = Wind speed at hub height (150m) in m/s
C_{100m} = Wind speed at reference height (100m) in m/s
z_{150m} = hub height = 150m
z_{100m} = reference height = 100m
$\alpha_{shear} = 0.11$ for offshore conditions [26].

Considering that the yaw control of the wind turbine is able to align the rotor towards the main wind speed direction, the wind speed velocity is obtained from the horizontal wind speed components (u and v) using Eqn. (2).

$$w = \sqrt{u^2 + v^2} \tag{2}$$

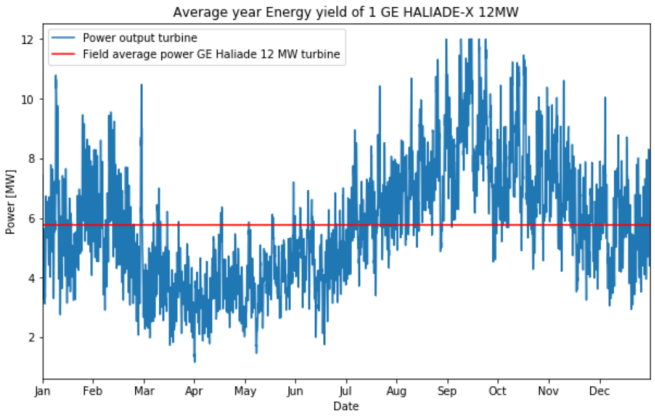

FIGURE 3. HOURLY POWER OUTPUT OF A SINGLE GE HALIADE-X 12 MW TURBINE FOR THE AVERAGE YEAR.

The average wind speed is around 8.5 m/s, indicating low to medium wind speeds in the area, with even lower values in the months from March to June. From a wind turbine selection perspective, low cut-in and rated wind speeds are preferable for the particular site conditions, which are more feasible for turbines with a large rotor diameter [27]. Furthermore, bigger turbines are also desirable for allowing a smaller number of units and consequently a smaller number of mooring lines and electrical cables, making it easier to be installed in an oil field that already has several sub-sea equipment. Despite the higher cost of bigger turbines, they also present possible cost reductions provided that they represent less than 30% of the CAPEX of an installed floating wind park [28].

After considering several commercially available wind turbines with oversized rotors, the 12 MW GE Haliade-X was selected, as it offers one of the lowest cut-in and rated wind speeds at 3 and 12 m/s respectively. Using the average year wind speeds in combination with the turbines's power curve [29], Fig. 3 was computed. This graph indicates that the turbine is not in an optimal location as the capacity factor is below 0.50. The power output is even lower from March to June where the capacity factor for those months is only 0.33. The occurring wind speeds below rated wind speed conditions can explain the significant fluctuations in power output for different months as shown in Tab. 1.

The dynamics of a floating turbine could impact the power production at the sub-minute time scale. To take that impact into account, not only a dynamic model is required but also a detailed description of the wind and wave characteristics that need to be obtained on the installation location. In addition, the power curve cannot give instantaneous power production but gives 10 min average values, which are enough to get insight within the scope of dimensioning the proposed storage system.

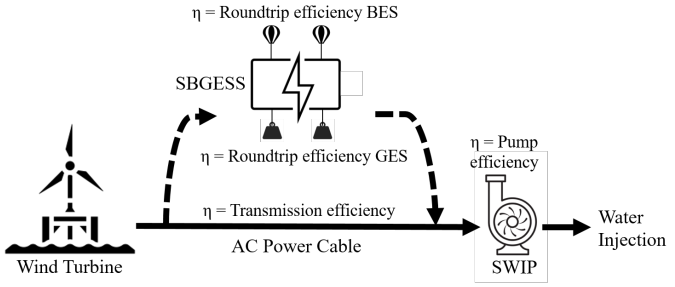

FIGURE 4. VISUAL OUTLINE OF SYSTEM COMPONENTS, INCLUDING POWER CONVERSION EFFICIENCY.

Energy demand

In order to select required energy storage capacity, it is essential to include the system efficiency in the assessment. As the turbines could be installed far from each other, wake effects are not expected, so it is assumed that all losses within the wind turbine are accounted for in its power curve. The following energy losses are included in the simulation: losses from gravitational and buoyancy energy storage, transmission losses and energy losses in the water pumps. For both GES and ByES, the round-trip efficiency (one complete cycle of charging and discharging) depends on many aspects, such as the velocity, shape and electrical equipment used. However, based on the values stated in [7, 16, 18, 30], 0.83 is used as round-trip efficiency for both GES and ByES. For the transmission losses in the power cables, a typical value of 0.975 used for short-distance (1-2km) inter-array three-core MVAC cables in the offshore wind industry [31] is adopted in this work. This value includes all transmission losses between the turbine and the pump. More accurate power losses in the cables can be described for different current and power levels, however detailed information on cable parameters is required [32]. Finally, the pump efficiency is included based on its operating envelope as a function of to the angular velocity and power level. A conservative approximation of the mean value resulted in an efficiency of 0.80 [21].

Two paths for the energy use are distinguished, the first one directly powering the SPRINGS, where only the cable and pump losses are considered, and the second one, which uses the storage system SBGESS in between. These two paths are visualised in Fig. 4. If the use of energy storage at a particular moment is unnecessary, the power losses are reduced as the storage losses are avoided. The simulation accounts for either path according to the specific situation .

The volumetric flow rate from the pump is computed through the so called P-Q curve. This curve uses the power, P_{OUT}, corrected for the losses in the pump to calculate the flow rate Q, injected in the seabed. In practice, the rate of water injection can be adjusted by means of a variable speed drive. As the range of rotational speeds is known, Eqn. (3) and (4) are com-

TABLE 1. STATISTICAL ANALYSES OF MONTHLY POWER OUTPUT FOR A 12MW HALIADE-X GE TURBINE, BASED ON 41 YEARS OF HOURLY WIND SPEEDS [25].VALUES ARE IN MW.

	Jan	Feb	Mar	Apr	May	Jun	Jul	Aug	Sep	Oct	Nov	Dec
Mean	6.25	6.25	4.73	4.48	4.77	5.3	6.3	7.11	7.41	6.98	6.41	5.97
STD	4.65	4.63	4.24	4.1	4.28	4.35	4.45	4.5	4.51	4.57	4.64	4.6
Min	0	0	0	0	0	0	0	0	0	0	0	0
25%	1.58	1.59	0.86	0.88	0.88	1.21	2.06	2.73	3.01	2.53	1.78	1.46
50%	5.92	5.93	3.53	3.18	3.47	4.34	5.96	7.62	8.28	7.17	6.07	5.26
75%	12	12	8.16	7.52	8.35	9.4	11.79	12	12	12	12	12
Max	12	12	12	12	12	12	12	12	12	12	12	12

bined to compute related P and Q values [33]. The subindex BEP stands for the best efficiency point.

$$\frac{Q}{Q_{BEP}} = \frac{n}{n_{BEP}} \tag{3}$$

$$\frac{P}{P_{BEP}} = \left(\frac{n}{n_{BEP}}\right)^3 \tag{4}$$

Where:

Q = Water injection flow rate

P = Shaft power

n = rotational speed of the pump

It should be noted that the BEP values at 4440 rpm for the power and flow rate correspond to 2170 kW and 278.23 m^3/h (42000 BPD) respectively [21]. Using Eqns. (3) and (4) the values at the lower bound of the rotational speed of 1500 rpm correspond to a power of 80.37 kW and a flow rate of 94 m^3/h. This procedure was done for 100 values, after which a P-Q curve was adjusted by a third-degree polynomial function presented in Eqn. (5).

$$Q_{system} = N(aP^3 + bP^2 + cP + d) \tag{5}$$

Q_{System} = total water injection flow rate

N = total number of pumps (2x)

a, b, c, d = polynomial fit coefficients

The coefficient of determination of the fitted curve is 0.998, and the curve fit is shown in Fig. 5. The resulting polynomial fit coefficients for a, b, c and d are $2.58\text{x}10^{-8}$, $-1.18\text{x}10^{-4}$, 0.227 and 82.581.

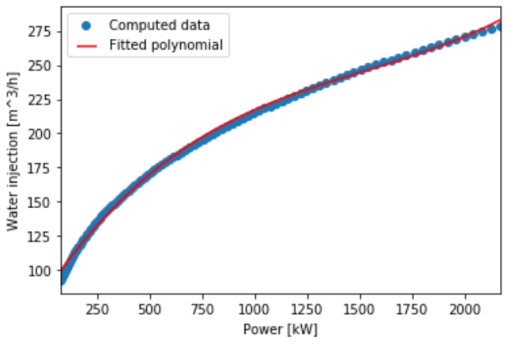

FIGURE 5. FITTED PUMP PERFORMANCE CURVE PLOTTED OVER COMPUTED DATA

.

Control strategy

Considering the resulting average annual capacity factor of 0.48 and the individulal component efficiencies described previously, at least two wind turbines are required to power a SWIP with two pumps with an average annual flow of 496.85 m^3/h. Nevertheless, considering the high seasonal monthly variability, as seen in Tab. 1, and the hourly power fluctuations, a control strategy needs to be defined in order to meet the average flow and the maximum number of starts targets with an adequate energy storage capacity. To conciliate these two targets, the control system will maintain the pumps working at maximum capacity as long as possible and enter a power-saving mode to keep the pumps running when the energy storage capacity reaches a minimum level (E_{SM}). The minimum energy storage capacity is obtained from the minimum pump power input and the required number of operation hours in energy-save mode (t_{SM}). A control strategy with three modes and a power-saving sub-mode is proposed and described below:

Mode 1: When the power generated by the wind turbines is

higher than the sum of P_{BEP} and the transmission losses, the power from the turbines is supplied directly to the pumps. All remaining power will be used for energy storage in the SBGESS until its total capacity is reached.

Mode 2: When the power generated by the wind turbines is within the power demand of the pumps (including losses), the power of the turbines is supplied directly to the pumps. Whether or not the SBGESS will be used to complement the power supply to the upper limit depends on which sub-mode is active:

Sub-mode 2a: When the SBGESS stored capacity is higher than E_{SM}, the SBGESS will be used to supply the additional power needed for the pumps to operate at their nominal capacity.

Sub-mode 2b: When the SBGESS stored capacity is equal or less than E_{SM}, the SBGESS will be in 'power-saving mode'. The SBGESS will only be used to avoid pump stops (e.g. act if mode 3 is active). This mode will automatically end once the storage capacity exceeds 20%. The pumps will operate at the power level that the wind turbines can supply.

Mode 3: When the power generated by the wind turbines is lower than the sum of P_{min} and the transmission losses, again two sub-modes can be identified:

Sub-mode 3a: When the power generated by the wind turbines combined with the power that the SBGESS can supply is enough to keep the pumps running at their minimum capacity, this will be done.

Sub-mode 3b: When the power generated by the wind turbines combined with the power that the SBGESS can supply is not enough to reach P_{min} and the transmission losses, the pump will shut down. The water injection rate will be zero, which will count as one stop. In this interval, any power generated by the wind turbine will be stored in the SBGESS.

Water injection simulation set-up

The aforementioned control strategy was implemented in a simulation environment to calculate the hourly flow curve and the total number of stops. The input parameters are the hourly power curve, system efficiencies, water injection flow function (Eqn. (5)), the total energy storage capacity of the SBGESS, and the number of hours set on the energy-save mode (t_{SM}). An iterative process was adopted to set the optimum values for the SBGESS capacity and (t_{SM}) that fulfil the required average flow according to the maximum number allowed of stops per year.

Design assumptions

The energy storage capacity is used as input parameter to assess the preliminary dimensions of the SBGESS. The design of the SBGESS is inspired by the design of the buoy supporting riser (BSR) developed by Petrobras and Subsea7 [34, 35]. The BSR is similar to the SBGESS as it is installed at a significant depth below sea level in the ultra-deep waters of Brazil and has connections to both topside and seabed. Although this design will be used as a basis for the main structure of the SBGESS, there are also significant structural differences. Most importantly, the BSR is asymmetrical due to the loading distribution of the risers' vertical forces concentrated on one end. The SBGESS will be shaped symmetrically as the vertical load distribution is mostly uniform. Another essential difference is that the risers and other elements of the BSR are all connected to the main ballasting section. For the SBGESS, most elements excluding the anchoring lines will be connected to the structural elements between the two main ballasting parts.

The total water depth at the installation location is assumed to be 2100 m, and the system will be installed at 1050 m allowing a (char)discharging distance of 1000 m for both GES and ByES. The ballasting tanks will be pressurised according to the water depth, reducing the static loading over the structure.

The length and width of the structure as well as the total ballasting tank volume are assumed to be nearly the same as the BSR. The mooring system type will be tension-leg, similar to the BSR. Materials and other structural details are not within the scope of this study, but an approximation of the total mass is made. The weights and floaters have a cylindrical geometry to minimise vortex-induced vibration and drag forces. The dynamic behaviour of these components will not be addressed at this stage of the project.

The sizing started with the power requirement. The required power supply by the SBGESS is not equal to the maximum power demand of the pump for two reasons. First, the electrical power cable and energy storage losses should be included. These losses are included considering that the cable connecting the wind turbines and the SWIP to the SBGESS has the same length and that the power supply accounts for half of the total storage cycle losses. Secondly, because of the control strategy defined with several modes, the energy storage should, in the most critical case, only deliver the power difference between the pumps power input at the best efficiency point and its minimal operational power. These two points are implemented in Eqn. (6). This equation includes the power cable and energy storage efficiencies η_T and η_{ES} while excluding the pump efficiency, as it was already included in the pump's power demand.

$$P = N \frac{P_{BEP} - P_{min}}{\sqrt{\eta_{ES}}\sqrt{\eta_T}} = 2P_{unit} \tag{6}$$

Equation 6 leads to the SBGESS requirement to supply at least 4.65 MW. As a design assumption, the SBGESS should be able to supply this amount of power by using only one energy storage module. The dimensions of both the weights and

the floaters will be selected to satisfy the required power supply. Hereafter, the total number of ESMs can be determined based on the total energy storage capacity (ES_{cap}) according with eq. (7).

$$ES_{cap} = N_{units} P_{unit} \frac{L}{v} \tag{7}$$

Where L is the available distance for the operation of weights and floaters and the N_{units} is the number energy of energy storage units, that is set as a multiple of four due to the symmetry of the SBGESS. v is the vertical velocity of the weights and floaters considered at 1 m/s, within the maximum efficiency range.

GES: weights dimensions

Equation (8) can be used to calculate the required mass for one weight. Hereafter the volume and the height of the weight can be obtained by using Eqns. (9) and (10). The mass of cables and supporting structures is neglected, and the weights are assumed to be made of high-density concrete.

$$m_{weight} = \frac{P_{unit}}{gv} \tag{8}$$

$$V_{weight} = \frac{m_{weight}}{\rho_c} \tag{9}$$

$$h_{weight} = \frac{V_{weight}}{\pi r^2} \tag{10}$$

m_{weight} = Mass of 1 weight unit in kg
g = gravitational acceleration in m/s^2
V_{weight} = Volume of a single weight unit in m^3
ρ_c = Density of concrete = 3400 kg/m^3 [36]
h_{weight} = Height of a single weight unit in m
r = Radius of the weight and floater units in m

A minimum distance of one diameter between the energy storage elements (weights and floaters) is required to avoid impacts during operation. So the radius of these elements will be selected as a function of the number of ESMs.

ByES: floaters dimensions

Equation (11) is used to obtain the required vertical force for a single floater. Assuming similar velocities and power supplied by weights and floaters, the volume and the height of the floater can be calculated through Eqn. (12) and (13). The floaters consist of Styrofoam, which is a lightweight material with a relatively low drag coefficient [17].

TABLE 2. MEAN WATER INJECTION FLOW RATE (m^3/h) AS A FUNCTION OF THE ENERGY STORAGE CAPACITY AND POWER-SAVING MODE TIME .

	6 h	12 h	18 h
6 MWh	502.50	502.29	501.90
8 MWh	504.04	503.88	503.54
10 MWh	505.49	505.34	505.05

$$F_{floater} = \frac{P_{unit}}{v} \tag{11}$$

$$V_{floater} = \frac{F_{floater}}{g(\rho_{sw} - \rho_{sf})} \tag{12}$$

$$h_{floater} = \frac{V_{floater}}{\pi r^2} \tag{13}$$

$F_{floater}$ = Net vertical force of a single floater unit in N
$V_{floater}$ = Volume of a single floater unit in m^3
ρ_{sw} = Density of seawater = 1030 kg/m^3 [37]
ρ_{sf} = Density of Styrofoam = 50 kg/m^3 [38]
$h_{floater}$ = Height of a single floater unit in m

RESULTS AND DISCUSSION

The power-safe mode greatly affects the number of stops along the year, allowing a continuous operation of the SWIP. Without this mode, 16 MWh of energy storage capacity is required to attend the required maximum number of stops per year, while only 2 MWh is required with 16 hours of t_{sm}. On the other hand, the ES_{CAP} is more relevant to determine the mean water injection flow rate. A summary of the sensitivity analyses of these parameters is shown in Tab. 2. The adoption of t_{SM} values above 12 hours do not bring additional benefits related to the reduction in the number of stops and impose a small reduction in the flow rate. This reduction is caused by the increase in the time the pumps will operate at minimum power. For each increment of 2 MWhr in the ES_{CAP}, an increase in the average flow of approximately 1.5 m^3/h is observed independently of the selected t_{SM}.

As a result of the iterative optimisation process, the values of 12 hours of power-saving mode and 8 MWh of energy storage capacity were obtained. The detailed results of this combination are shown in the histograms and adjusted probability density functions for the average hourly flow rate and the yearly number of stops shown in Figs. 6 and 7.

The water injection flow rate requirement is satisfied from the resulting average value of 503.88 m^3/h. Yet it is observed that the conditions are not met for all the years in the sample. The

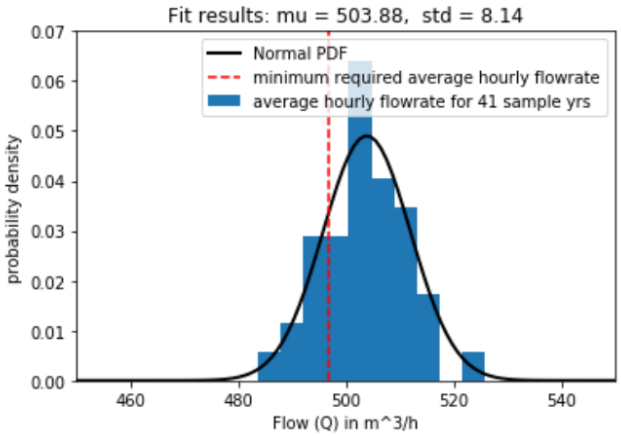

FIGURE 6. HISTOGRAM OF AVERAGE HOURLY FLOW RATE INCLUDING A FITTED NORMAL DISTRIBUTION PDF.

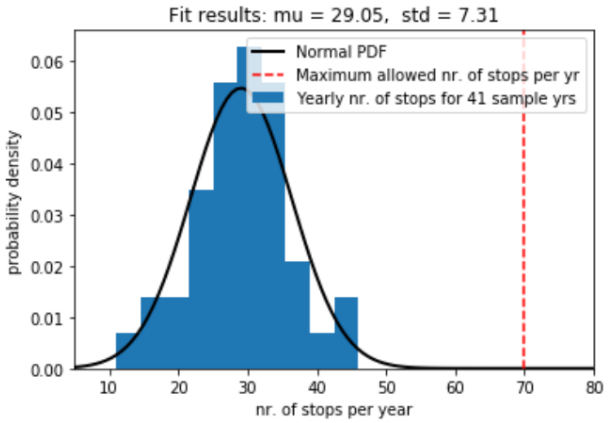

FIGURE 7. HISTOGRAM OF THE NUMBER OF YEARLY STOPS INCLUDING A FITTED NORMAL DISTRIBUTION PDF.

probability of the average injection rate being below the required value for a certain year is 19.4%. However, the year with the lower average injection rate is 3% below the target value and that the mean flow over the project lifetime is reached. The maximun number of stops requirement is met as all 41 sample years have a total amount below 70 yearly stops. The probability of exceeding the maximum stops per year is negligible, while the probability of exceeding at least 50 stops is $2.1\text{x}10^{-3}$. This is deemed as an acceptable risk. A summary of these results is shown in Tab. 3.

In the proposed approach to obtain the required energy storage capacity, several assumptions and simplifications were employed in the simulation model. The fitted distributions accounted equally for the forty-one years of data. Thus, regional effects such as El Niño/La Niña, but also global events such as climate change could mean that recent shifts in wind patterns [39, 40] have a less prominent effect in the distributions

TABLE 3. RESULTS OF THE SIMULATION OF THE WATER INJECTION SYSTEM, FOR FORTY-ONE YEARS OF DATA.

Results	Value
Mean & STD nr. of stops per year	29.05 / 7.31
Probability of exceeding 50 stops per year	$2.1\text{x}10^{-3}$
Mean & STD water injection	503.88 / 8.14
Probability of insufficient injection	0.194
Energy storage capacity (EScap)	8 MWh
Power-saving mode time	12 hours

than they would have if only recent years were considered. Another assumption is based on the selection of a normal distribution to describe the hourly results. Thus, besides the entire forty-one sample years, each sample year was checked individually to comply with the operational requirements. Other probability distribution functions such as the Weibull distribution could also be used to obtain a more accurate representation of the results. Finally, the wind turbines and pumps were assumed to have full availability. In reality, the O&M strategies will have an important impact on the results due to the monthly variability of the wind resource; however, to correctly account for these effects, more specific information is needed.

Preliminary dimensioning of the SBGESS

A symmetrical shape of the semi-submerged support structure is proposed with an equal number of weights and floaters on both the front and back side of the SBGESS. An even number of units was selected with the purpose to simplify and derisk the installation process. In order to fulfill these requirements, a minimum number of 8 EMSs units are needed resulting in an energy storage capacity of 10.32 MWh. Besides the symmetry argument, an even number of chosen units also allows for a certain level of redundancy as the capacity would still be larger than 8 MWh, which is the minimum energy storage capacity required, in case one ESM is out of operation.

A schematic showing the configuration of the main structure is visualised in Fig. 8. An overview of the proposed dimension values for the SBGESS can be found in Tab. 4. With the selected velocity of 1 m/s, a minimum time of 16.7 minutes is required to obtain full energy storage capacity, considering that multiple ESMs could be charged at the same time. A total volume of 8998 m^3 is estimated for the ballast tanks.

The selected dimensions follow the basis of design with respect to the functionality of the SBGESS. By implementing the operational modes described in the control strategy section, it was assumed that the units are allowed to accelerate and decelerate fast enough to the required velocity and deliver the needed

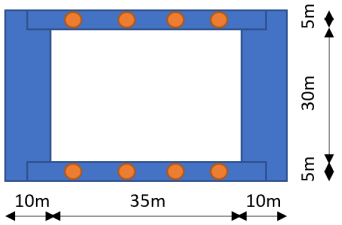

FIGURE 8. SCHEMATIC TOP VIEW OF THE SBGESS INCLUDING DIMENSIONS OF THE MAIN ELEMENTS

TABLE 4. PRELIMINARY DIMENSIONS OF THE SBGESS

Parameter	SBGEES	weights	floaters
Length [m]	55	-	-
Width/radius [m]	40	2.5	2.5
Height [m]	10	5.02	12.31
Number of units	1	8	8
Total mass [tonne]	2800	2681.6	96.65

amount of power. In reality, system dynamics will play an important role in imposing maximum and minimum allowable velocities, restricting the power range of the SBGESS. In addition, the system should allow for both sequential and simultaneous operation of parallel units depending on the specific requirements of power supply and demand.

CONCLUSION

In this paper, a methodology for the preliminary assessment of a subsea buoyancy and gravity energy storage system (SBGESS) was presented.The SBGESS is particularly interesting for deep and ultra-deep waters locations, where it can be applied to enable the use of renewable energies to power subsea equipment and to replace part of the fuel consumption in offshore platforms. The proposed solution can also contribute to increase the oil & gas production without increasing the number of oil platforms. The proposed energy storage system was designed to ensure that a seabed mounted water injection plant complies with the average water injection flow rate and the maximum number of annual shutdowns. This system has a similar size of an already installed buoy supporting riser, indicating that the installation of the SBGESS could take place with current technology. The proposed control strategy with three operation modes and a power-saving sub-mode allowed a reduction of the energy storage capacity required to meet the operational targets. Further work will address the dynamic behaviour of the floaters and weights and the O&M strategies' impacts on the energy storage capacity estimation and the control strategy.

ACKNOWLEDGMENT

This study was supported by PETROBRAS.

REFERENCES

[1] Wood Mackenzie, 2019. Why powering oil and gas platforms with renewables makes sense. Tech. Rep. October.

[2] Bacati, F., Arcangeletti, G., Breuskin, B., Giolo, R., Muguerra, P., Radicioni, A., Shaiek, S., and Sibaud, E., 2020. "How Technology Enables A Lower Cost for Subsea Tiebacks". In Proceedings of the Annual Offshore Technology Conference, Vol. May.

[3] Hawthorn, K., Mclaurin, D., Thomas, L., Cowin, T., Ocando, M., Albaugh, E. K., Davis, D., and Jones, C., 2020. "2020 Worldwide Survey of Subsea Processing Poster". *Offshore magazine*.

[4] Giolo, R., Berthelot, A., Pedenaud, P., and Skivington, G., 2019. "Industrialisation of Springs, a qualified subsea sea water desulfation process". *Proceedings of the Annual Offshore Technology Conference,* ***May***.

[5] Mauries, B., Arcangeletti, G., Colmard, C., Di Felice, A., Delahaye, T., La Sorda, E., D'Amico, A., and Temeng, K.-G., 2020. "Floating Offshore Windfarm Integrated in the Subsea Field - Saipem Windstream Concept, Applied to a Case Study Benjamin". In Offshore Technology Conference 2020.

[6] Equinor, 2020. Hywind Tampen - floating wind power project.

[7] Wang, Z., Carriveau, R., Ting, D. S., Xiong, W., and Wang, Z., 2019. "A review of marine renewable energy storage". *International Journal of Energy Research,* ***43***, pp. 6108–6150.

[8] Dündar, G., 2012. "Design and Manufacture Study of Ocean Renewable Energy Storage (ORES) Prototype". PhD thesis, Massachusetts Institute of Technology.

[9] Puchta, M., Bard, J., Dick, C., Hau, D., Krautkremer, B., Thalemann, F., and Hahn, H., 2017. "Development and testing of a novel offshore pumped storage concept for storing energy at sea - Stensea". *Journal of Energy Storage,* ***14***, pp. 271–275.

[10] Cazzaniga, R., Cicu, M., Marrana, T., Rosa-clot, M., Rosa-clot, P., and Tina, G., 2017. "DOGES : Deep ocean gravitational energy storage". *Journal of Energy Storage,* ***14***, pp. 264–270.

[11] Germa, J.-M., Delbosc, C., Perez, R., Monluc, B., Colléter, M., Hontebeyrie, N., and Garbay, M. MGH - Clean energy for the seas.

[12] Luo Z, Tian Y, Huang L, Yang F, L. B., 2016. A gravity energy storage system using ocean depth difference.

[13] Noble, G., 2017. Sink Float Solutions : un démonstrateur peut-être en test en 2018.

[14] Saragossi, R., 2018. Sink Float Solutions: Assessing the

feasibility of an energy storage solution. Tech. rep., ENGIBEX.

[15] Klar, R., Steidl, B., and Aufleger, M., 2018. "A floating energy storage system based on fabric". *Ocean Engineering,* ***165***(December 2017), pp. 328–335.

[16] Bassett, K. P., Carriveau, R., and Ting, D. S., 2017. "Integration of buoyancy-based energy storage with utility scale wind energy generation". *Journal of Energy Storage,* ***14***, pp. 256–263.

[17] Alami, A. H., 2020. "Buoyancy Work Energy Storage (BAES) Systems". In *Mechanical Energy Storage for Renewable and Sustainable Energy Resources*. Springer, Cham, Switzerland, pp. 87–92.

[18] Morgan, E. A., 2010. Buoyancy energy storage and energy generation system U.S. Patent 2010/0107627 A1.

[19] Chetwynd, G., 2016. "Brazilian battle on to slash costs across the board". *upstream - the international oil & gas Newspaper - FOCUS BRAZIL*, pp. 32–33.

[20] Chetwynd, G., 2016. "Turning a problem into an advantage". *upstream - the international oil & gas Newspaper - FOCUS BRAZIL*, pp. 32–33.

[21] Petrobras, 2020. Petrobras internal communication.

[22] Stover, D. L., and Travaini, L., 2019. "Barrier fluidless, sealless seawater canned motor pumps". *Proceedings of the Annual Offshore Technology Conference,* ***May***, pp. 6–9.

[23] Novgorodcev Jr., A. R., and Jarquín-Laguna, A., 2021. "Multi-criteria analysis to rank offshore renewable technologies to support deep-water oil and gas production". In Developments in Renewable Energies Offshore - Proceedings the 4th International Conference on Renewable Energies Offshore, RENEW 2020, S. S.C., ed., CRC Press/Balkema, pp. 771–778.

[24] The Copernicus Climate Change Service (C3S), 2020. ERA5: Fifth generation of ECMWF atmospheric reanalyses of the global climate.

[25] Hersbach, H., Bell, B., Berrisford, P., Biavati, G., Horányi, A., Muñoz Sabater, J., Nicolas, J., Peubey, C., Radu, R., Rozum, I., Schepers, D., Simmons, A., Soci, C., Dee, D., and Thépaut, J.-N., 2018. Era5 hourly data on single levels from 1979 to present. copernicus climate change service (c3s) climate data store (cds). accessed on 01-12-2020; 10.24381/cds.adbb2d47.

[26] Emeis, S., and Turk, M., 2007. "Comparison of logarithmic wind profiles and power law wind profiles and their applicability for offshore wind profiles". In Wind Energy, J. Peinke, P. Schaumann, and S. Barth, eds., Springer Berlin Heidelberg, pp. 61–64.

[27] Enevoldsen, P., and Xydis, G., 2019. "Examining the trends of 35 years growth of key wind turbine components". *Energy for Sustainable Development,* ***50***, June, pp. 18–26.

[28] DNV GL, 2020. Bankability of floating wind projects. Tech. Rep. June, Haugesund.

[29] ASA BRANCA USINAEOLICA, 2019. Requerimento eb-2-2019; 48513.010255/2019-00.

[30] Toubeau, J. F., Ponsart, C., Stevens, C., De Grève, Z., and Vallée, F., 2020. "Sizing of underwater gravity storage with solid weights participating in electricity markets". *International Transactions on Electrical Energy Systems*(June), pp. 1–17.

[31] Madariaga, A., Martín, J. L., Zamora, I., Ceballos, S., and Anaya-Lara, O., 2013. "Effective assessment of electric power losses in three-core xlpe cables". *IEEE Transactions on Power Systems,* ***28***, pp. 4488–4495.

[32] Mokhi, C. E., and Addaim, A., 2020. "Optimization of wind turbine interconnections in an offshore wind farm using metaheuristic algorithms". *Sustainability (Switzerland),* ***12***, 7, pp. 1–24.

[33] Pöyhönen, S., Ahonen, T., Ahola, J., Punnonen, P., Hammo, S., and Nygren, L., 2019. "Specific speed-based pump flow rate estimator for large-scale and long-term energy efficiency auditing". *Energy Efficiency,* ***12***, 6, pp. 1279–1291.

[34] Cruz, I., Claro, C., Sahonero, D., Otani, L., and Pagot, J., 2015. "The buoy supporting risers (bsr) system: A novel riser solution for ultra-deep water subsea developments in harsh environments". *Offshore Technology Conference*, October.

[35] van Diemen, J., Saint-Marcoux, J., Otani, L., Sahonero, D., and Cerqueira Trovoado, L., 2015. "Displacing 10,000t of water to install 2,500t of steel buoy at 250m below sea level". *Offshore Technology Conference*, May.

[36] Leung, C., 2001. "Concrete as a building material". In *Encyclopedia of Materials: Science and Technology*, K. J. Buschow, R. W. Cahn, M. C. Flemings, B. Ilschner, E. J. Kramer, S. Mahajan, and P. Veyssière, eds. Elsevier, Oxford, pp. 1471–1479.

[37] García-Abdeslem, J., 2020. "On the seawater density in gravity calculations". *Journal of Applied Geophysics,* ***183***, 12.

[38] Liu, P., and Chen, G., 2014. "Chapter eight - applications of polymer foams". In *Porous Materials*, P. Liu and G. Chen, eds. Butterworth-Heinemann, Boston, pp. 383–410.

[39] Greene, S., Morrissey, M., and Johnson, S. E., 2010. "Wind climatology, climate change, and wind energy". *Geography Compass,* ***4***, 11, pp. 1592–1605.

[40] Lima, D. K., Leão, R. P., dos Santos, A. C., de Melo, F. D., Couto, V. M., de Noronha, A. W., and Oliveira, D. S., 2015. "Estimating the offshore wind resources of the state of ceará in brazil". *Renewable Energy,* ***83***, 11, pp. 203–221.